View metadata, citation and similar papers at core.ac.uk
brought to you by CORE
provided by Chalmers Publication Library

Cold cathode emission studies on topographically modified few layer and single layer MoS_2 films

Anand P. S. Gaur,[1] Satyaprakash Sahoo,[1,2,a),b)] Frank Mendoza,[1] Adriana M. Rivera,[1] Mohit Kumar,[2] Saroj P. Dash,[3] Gerardo Morell,[1] and Ram S. Katiyar[1,b)]
[1]*Department of Physics and Institute for Functional Nanomaterials, University of Puerto Rico, San Juan, Puerto Rico 00931, USA*
[2]*Institute of Physics, Bhubaneswar 751005, Odisha, India*
[3]*Department of Microtechnology and Nanoscience, Chalmers University of Technology, SE-41296, Göteborg, Sweden*

(Received 27 August 2015; accepted 5 January 2016; published online 26 January 2016)

Nanostructured materials, such as carbon nanotubes, are excellent cold cathode emitters. Here, we report comparative field emission (FE) studies on topographically tailored few layer MoS_2 films consisting of $\langle 0001 \rangle$ plane perpendicular ($\perp$) to *c*-axis (i.e., edge terminated vertically aligned) along with planar few layer and monolayer (1L) MoS_2 films. FE measurements exhibited lower turn-on field E_{to} (defined as required applied electric field to emit current density of 10 μA/cm^2) $\sim$4.5 V/μm and higher current density $\sim$1 mA/cm^2, for edge terminated vertically aligned (ETVA) MoS_2 films. However, E_{to} magnitude for planar few layer and 1L MoS_2 films increased further to 5.7 and 11 V/μm, respectively, with one order decrease in emission current density. The observed differences in emission behavior, particularly for ETVA MoS_2 is attributed to the high value of geometrical field enhancement factor (β), found to be $\sim$1064, resulting from the large confinement of localized electric field at edge exposed nanograins. Emission behavior of planar few layers and 1L MoS_2 films are explained under a two step emission mechanism. Our studies suggest that with further tailoring the microstructure of ultra thin ETVA MoS_2 films would result in elegant FE properties. © *2016 AIP Publishing LLC*. [http://dx.doi.org/10.1063/1.4940306]

The cold cathode emitters based technologies, such as flat displays,[1] vacuum microelectronics,[2] x-ray sources,[3,4] and electron guns,[5] requisite coherent electron emission and high current density at low turn-on field (E_{to}). For this purpose, the best-preferred metal emitters are engineered in the form of a sharp pointed[6] source to subdue E_{to} further. In such emitters, due to the presence of the large gradient of localized electric field at the pointed/sharp surface, there is a significant improvement in the emission current density. Analogous to this, materials with tailored structures, such as tubes,[7–9] sheets,[10] ribbons,[11] and wires,[12,13] also exhibit elegant field emission (FE) behavior. For example, field emitters consisting of the vertically aligned carbon nanotubes (CNTs) array have recently been exploited in microwave diode[2] and electron gun[5] applications. Along with CNT other carbon nanomaterials, such as graphene, nanodiamonds, and nanoribbons, were also studied for cold cathode emission. Atomically thin, two-dimensional (2D) monolayer graphene has many novel properties,[14,15] but contrary to the CNT, magnitude of E_{to} for monolayer graphene was found to be quite high, and therefore potentially hinders its FE application. However, studies on the edges of graphene sheet (with exposed C atoms having incomplete C-C bonds) have shown enhanced FE behavior with extremely low E_{to}, which is ascribed to the lower work function of edges,[16] and similar observations were reported for graphene flakes[17] and doped graphene.[18]

Recently, other 2D materials, particularly the transition metal dichalcogenides (TMD) family, have received much attention owing to their thickness dependent wide range of electrical, electronic, and optoelectronic properties. Among these, monolayer (1L) MoS_2 has triggered much attention for its exciting physical properties.[19–22] The anisotropy in chemical bonding in MoS_2 sheets results in active edges similar to graphene sheet edges. In recent developments, synthesis of large area MoS_2 film with edge terminated vertically aligned (ETVA) layers via sulfurization of molybdenum film in sulfur environment[23,24] has been reported. However, unlike carbon materials, MoS_2 has not been explored much for FE.

In the present work, we focus on the FE properties of few layers of planar, ETVA, and monolayer MoS_2 films. Our studies revealed that the MoS_2 films containing ETVA layers exhibit lower E_{to} and higher geometrical field enhancement factor (β) than planar few layer and monolayer MoS_2 films. For 1L-MoS_2, turn on field was even more than that of planar few-layer MoS_2 films. FE behavior for ETVA MoS_2 films was correlated to its microstructure and the emission behavior for planar few layer and 1L-MoS_2 have been discussed under a serial two step emission process.

Synthesis of large area growth of ultrathin ($\sim$4–6 nm) planar and edge oriented, as well as monolayer MoS_2 films, has been reported earlier.[25] In brief, 1L and planar MoS_2 films were synthesized on SiO_2/Si substrates via chemical vapor deposition (CVD) and edge exposed MoS_2 films were synthesized by sulfurization of molybdenum coated SiO_2/Si substrates at two different temperatures given as 900 °C and 550 °C, respectively, in $H_2 + Ar$ atmosphere. Thickness and

a)Present address: Institute of Physics, Bhubaneswar 751005, India
b)Authors to whom correspondence should be addressed. Electronic addresses: rkatiyar@hpcf.upr.edu and satya504@gmail.com

microstructure of the few layer films were characterized in tapping mode atomic force microscopy (AFM-VEECO) and High Resolution Transmission Electron Microscopy (HRTEM JEOL JEM-2200FS) operated at 200 kV, respectively. Raman and photoluminescence (PL) spectroscopy were carried out using a Horiba-Jobin T64000 (triple mode subtractive) micro-Raman system in backscattering configuration utilizing an Argon ion laser (514.5 nm line as excitation source) for phase and 1L thickness confirmation of the grown MoS_2 films. Prior to FE measurements, MoS_2 films were transferred upon Pt/Si substrates by a wet chemical etching method reported elsewhere.[26] Field current was measured for all MoS_2 films in a diode configuration at pressure 1.5×10^{-7} m-bar in a custom made system.[27] A Stanford Research Systems PS350 and Keithley 6517A electrometer were used as the voltage source and current measurement, respectively, and emission current magnitude lower than 1×10^{-12} A was considered at the background noise, while E_{to} was defined as the required magnitude of applied electric field necessary to emit a current density of 10 μA/cm^2 following earlier reports on MoS_2.[28,29] However, in a few reports on carbon-based materials,[30] E_{to} was defined as to achieve emission current density of 1 nA/cm^2. To make meaningful comparisons with previous MoS_2 reports, we stick to 10 μA/cm^2 as E_{to}. The surface morphology and kelvin probe force microscopy (KPFM) of all layers were examined by *ex-situ* AFM (MFP-3D, Asylum Research) in lift mode using conductive Pt-coated tips (AC240TM, Electric-Lever, Olympus, with radius of curvature ~30 nm, stiffness ~2 N m^{-1}, and a resonance frequency of ~70 kHz).

Figure 1(a) shows the HRTEM image of few-layer MoS_2 film grown at low (500 °C) temperature. The microstructure exhibits distinct stripe-like features [enlarged image shown in Fig. 1(b)], distributed equally with flat, i.e., *c*-axis oriented nanocrystalline regions. The measured separation between two such stripes was found to be ~0.7 nm, which is the thickness of single layer MoS_2. This thickness corroborated that striped grains consist of vertically oriented (⊥ *c*-axis) layers of MoS_2. The measured film thickness and roughness were found to be ~7–8 nm and below 1 nm, respectively.[44] In contrast to edge exposed MoS_2 films, the MoS_2 films grown at higher temperature (at 900 °C) were well crystalline and contain only *c* axis oriented planes; this we have demonstrated in our earlier reports.[25] The difference in the microstructure between these two films explained under reaction kinematics has been reported elsewhere.[25]

Raman spectroscopy has been used to quantify different physical properties in MoS_2 such as the number of layers,[31] thermal conductivity,[32] crystallite size,[24] and doping concentration.[33] Figure 2(a) shows the room temperature Raman spectra of 1L, ETVA, and few-layer MoS_2 films. It can be seen from the figure that, for 1L-MoS_2, E^1_{2g}, A_{1g} modes blue and red shifted, respectively, with respect to their bulk frequencies, which will be discussed later. Broadening of phonon lineshape of these modes in ETVA MoS_2 film with respect to bulk MoS_2 film was noticed. Raman lineshape is very sensitive to crystallite size[34] and lattice disorder[35] and in nanomaterials due to phonon confinement and defects the phonon line shape exhibits asymmetry and broadening.

The observed broadening and line shape asymmetry in Raman bands in ETVA MoS_2 film can be ascribed to the presence of striped and *c*-axis oriented nanocrystalline grains. Moreover, the shift in frequency of these modes in 1L-MoS_2 with respect to few layer films is due to the alteration in in-plane bonding and Coulombic interaction between consecutive layers. In fact, the shift in frequency of these two modes with respect to bulk MoS_2 is used to determine the monolayer nature of MoS_2 and found to be in accordance with earlier reported results.[31] Further, the emergence of PL in MoS_2 has been used as the signature[36] of its 1L form. In our case, we obtained huge room temperature PL intensity, centered around 1.8 eV, which is shown in Fig. 2(b). This also confirms our MoS_2 thin film to be 1L. For comparison, PL spectra for few-layer MoS_2 is also shown in the figure. In contrast, there is no signature of a PL band in the few layer sample indicating its indirect band gap nature.

There are few reports on FE studies on chemically synthesized MoS_2 flakes[28] and flowers[29] like nanostructures. The reported E_{to} values were found to be lower in sheets, ~3.5 V/μm, while in nanoflowers, a high magnitude of emission current density ~10 mA/cm^2 at higher magnitude of electric field ~8 V/μm was reported. The demonstrated lower magnitude of E_{to} and high emission current density in flakes and nano flowers, respectively, were explained by considering the fact that the edges of MoS_2 account for the multifold increase in the localized electric field, and this resulted in higher emission current density. However, no such

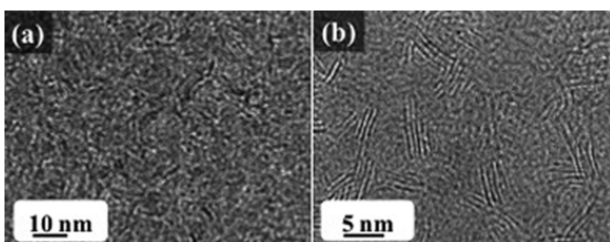

FIG. 1. (a) HRTEM image of ETVA MoS_2 film. (b) Magnified image showing clear vertically aligned layers.

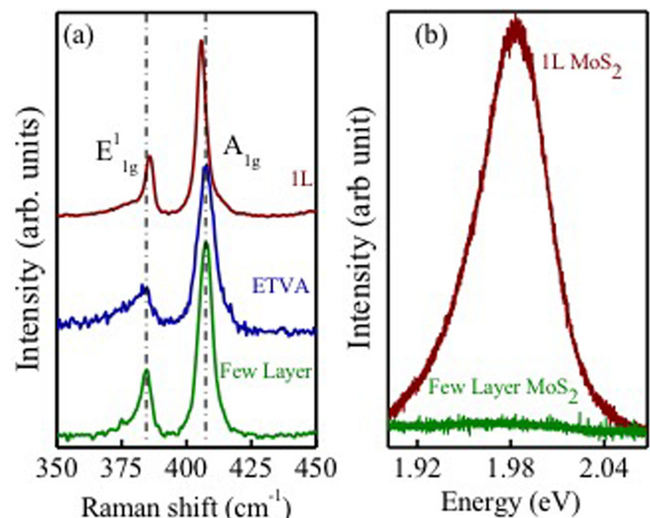

FIG. 2. (a) Raman spectrum of 1L, ETVA, and few layer MoS_2 film. (b) Photoluminescence spectrum of 1L and few layer MoS_2.

attempts have been made to understand the FE behavior in CVD grown large area MoS_2 films. In particular, thickness dependent FE studies are still lacking. Figure 3(a) represents the FE characteristic for few layer and 1L-MoS_2 films. These experimental results ascertained that 1L-MoS_2 has higher turn-on field $\sim$11 V/μm over the few layer form, which showed $E_{to} \sim 5.7$ V/μm. In general, Fowler-Nordheim (FN) theory, developed for metallic surface, has been used to analyze the electron emission. Accordingly, the relation for electron emission is $I \propto AE_{eff}^2 \exp(\frac{-B}{E_{eff}})$, where A and B are constants and E_{eff} is the localized electric field. Although in the case of semiconductor materials, Stratton[37] discussed the effect of surface states and lowering of the conduction band due to penetration of external field. But the implication of this mathematical expression for emission current density for real semiconductor material, particularly for mono or few-layer MoS_2, would be complicated and beyond the scope of the present study. In view of this, we analyze our results using Fowler-Nordheim formalism. J/E^2 versus 1/E plots shown in Fig. 3(b) for few-layer and 1L-MoS_2 films exhibit linear behavior with a negative slope for higher applied fields indicating the F-N type tunneling mechanism. In such cases, a rough approximated geometrical factor β for 1L and few- layer MoS_2 films can be obtained using the following equation:[28]

$$\beta = (6.8 \times 10^3 \times \phi^{\frac{3}{2}})/\mathrm{m}, \quad (1)$$

where m is the slope of fitted straight line and ϕ is work function. The estimated values of β were found to be 601 and 503 for few-layer and monolayer MoS_2 films, respectively, and are comparably low with the values for sheets and flowers. The higher magnitude of E_{to} and lower values of β in the present work further corroborated the smooth planar surface of 1L and few-layer MoS_2 films as planar geometry is not suitable to achieve a high geometrical enhancement factor. Further, the observed deviation from linear FN behavior in the J/E^2 versus 1/E plot in Fig. 3(b) at higher bias voltages is indicative of the semiconducting behavior of MoS_2 films.

In the present study, the observed differences in FE characteristics between the few-layer and single layer MoS_2 films can be described under two step electron emission mechanism first proposed by Binh *et al.,* for planar ultrathin ($\sim$5 nm) film of wide band gap n-type semiconductor.[38,39] In the first step, the electrons begin to inject into the semiconductor from the metal contact (in present case Pt) under the influence of applied external field, resulting in the space charge accumulation at the metal-semiconductor interface. With the building of the space charge, the band bending takes place in the semiconductor that allows electrons to tunnel directly into the conduction band from metal through the potential barrier as shown in the schematic diagram in Fig. 4(a). The constituted tunneling current is given by Shockley equation

$$J = AT^2\left(\exp^{\frac{-e\phi_b}{kT}}\right)\left[\exp^{\frac{eV_{eff}}{nkT}} - 1\right], \quad (2)$$

where k, ϕ_b, and V_{eff} are Boltzman constant, Schottky barrier height, and the potential difference across the semiconductor generated due to the applied field, respectively. At the beginning with lower fields, thermally active electrons are the only source that contributes to the space charge formation, as tunneling probability of electron through the barrier is negligible. Moreover, the Schottky barrier height at interface restricts the emission current and for higher values of ϕ_b, current density reduces further. Here, it is worth mentioning that our MoS_2 samples show n-type behavior.[44] For Pt-MoS_2 (few-layer) interface, the reported barrier height was estimated to be $\sim$0.2 eV (Ref. 20) and expected to increase further for monolayer MoS_2 due to opening up of the band gap. This accounts for lowering of the magnitude of emission current observed in monolayer MoS_2 at lower applied fields. In

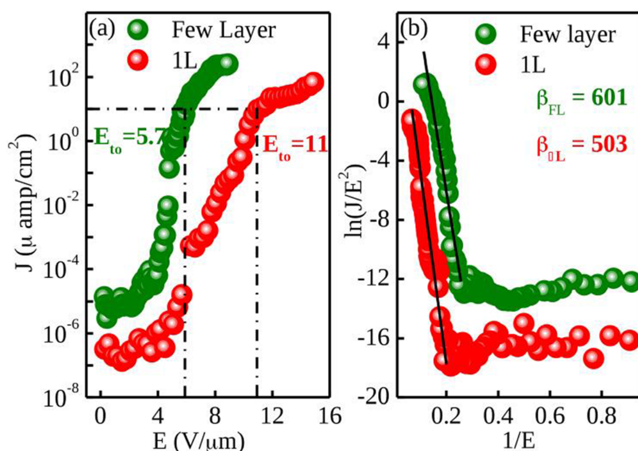

FIG. 3. (a) Field emission J-E curves. (b) FN plots for few-layer and 1L-MoS_2 films. Emission current was recorded keeping the detector at 100 μm away from emitting surface.

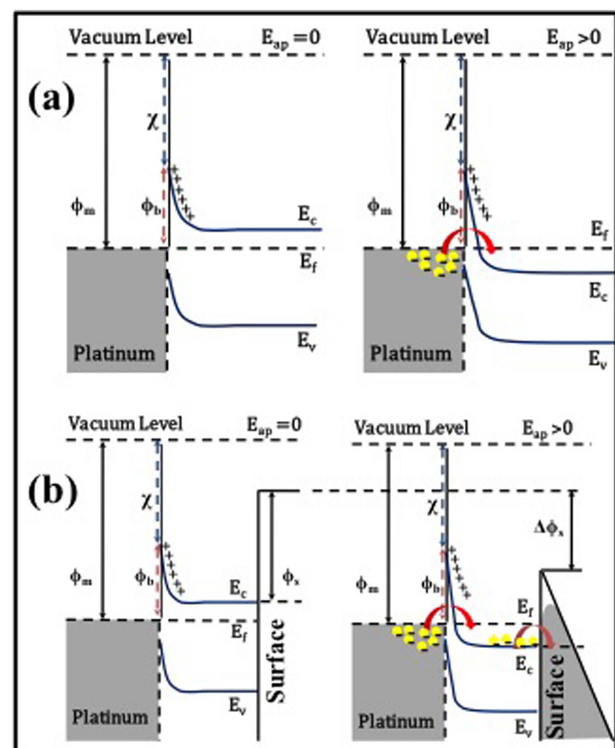

FIG. 4. Schematic of a two step emission mechanism. (a) Band bending at the metal-semiconductor interface in the presence of the applied field, when $E_{ap} > 0$ electrons from metal tunnel into the conduction band. (b) Surface barrier lowering followed by electron tunneling into the vacuum due to the lowering of the surface barrier shown in gray color.

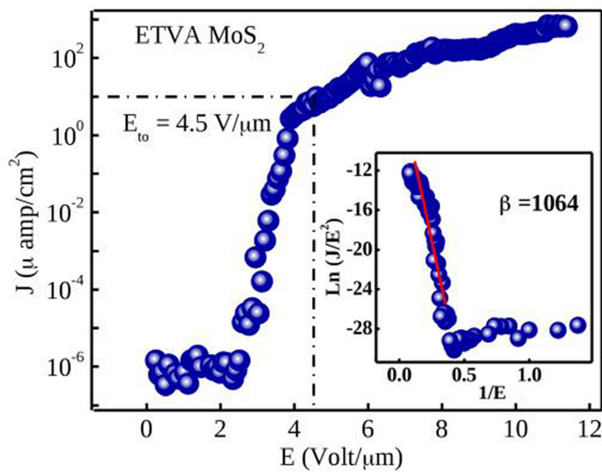

FIG. 5. FE J-V curves of edge exposed MoS_2 film, and inset shows the FN plot.

1L-MoS_2, other intrinsic factors such as higher effective mass and enhanced interactions among confined charge carriers might also contribute in the reduction of emission current.[40,41] Hence, the magnitude of semiconductor work function and space charges accumulated inside the semiconducting layer are also significant to achieve low threshold field. For this, we have evaluated the work functions for few-layers, ETVA, and mono layer MoS_2 using KPFM, which will be discussed later. A certain minimum thickness of the semiconductor is indeed necessary for building up space charge inside the layer. The theoretically estimated thickness for planar TiO_2 was found to be ∼4 nm and below this thickness increase in the concentration of space charge was found to be field independent.[38] Similarly, in the case of 1L-MoS_2 sufficient space charges were not able to be acquired due to ultra low thickness (0.7 nm), which in turn affected the band bending process. As a result, it requires higher fields for emission with respect to few-layer MoS_2. In the second step, simultaneously with band bending, under the effect of applied field, vacuum barrier is lowered due to Schottky effect and electrons begin to emit from the semiconductor surface into the vacuum as shown in the schematic of Fig. 4(b). It may be pointed out that the emission characteristic of planar MoS_2 samples is argued assuming the ideal condition surface without considering the surface states, roughness, and foreign contaminants.

Contrary to the planar structure, sharp edge geometry is preferred due to the large confinement of the localized electric field that showed lower turn-on field, with large emission current density. Figure 5 shows the FE behavior of EVTA MoS_2 film for which E_{to} was found ∼4.5 V/μm with higher numerical values of β (1064), extracted from linearly fitted I-V data at a higher electric field utilizing Eq. (2). For the β calculation magnitude of work function for edge exposed MoS_2 was estimated to be ∼4.18 eV using KPFM.

The emission current density showed significant improvement and was found to be ∼1 m-A/cm^2. Similar enhanced FE behavior has been reported for other solids consisting of nano-protrusions. The surface of MoS_2 film containing oriented layers has average roughness below 1 nm, which could also be realized by the contrast of the HRTEM image shown in Fig. 1(a), confirming that stripe like grains were not extended beyond the flat surface, thereof, the observed value of E_{to} and emission current magnitude might differ from MoS_2 nanoflowers to sheets.

Other factors, such as the work function of the vertically aligned MoS_2 layers, might be different and, hence, could have significant contributions in emission behavior. To further understand the obtained field emission results for few-layers of planar, monolayer MoS_2, and EVTA films in terms of their work functions, KPFM was used to evaluate the work functions. It may be pointed out that KPFM is considered to be a suitable non-contact technique and has been used to map the two-dimensional distributions of contact potential difference (V_{CPD}) between the tip and a sample. The V_{CPD} can further be exploited to evaluate the work function (Φ_{sample}) of the material through the following mathematical equation:[42]

$$\Phi_{sample} = \Phi_{tip} - eV_{CPD}, \quad (3)$$

where Φ_{tip} and e are the work function of the AFM tip and electronic charge, respectively.[42,43] The work function of the tip used in the present study (Si coated with Pt/Ir) is $\Phi_{tip} = 4.45$ eV.

The measured two-dimensional distributions of contact potential difference (V_{CPD}) of few-layers of planar, monolayer MoS_2, and ETVA films are shown in Figures 6(a)–6(c). Using Eq. (3), the work function of the few-layers of planar, monolayer MoS_2, and ETVA films are found to be ∼4.39, 4.82, and 4.18 eV, respectively. This result suggests that the lowest value of work function for ETVA also accounts for its improved FE performance as compared with few-layer and mono layer MoS_2 thin films.

Hence, ultra thin ETVA-MoS_2 films have shown cold emission characteristics in the proximity of other carbon-based materials. Moreover, the sulfurization method has adequate space to improve the density of such edge exposed MoS_2 films (Ref. 23) to tune the emission behavior further. The field emission stability was monitored over a period of 12 h for the emission current density at 500 and 150 μA/cm^2 for ETVA and few-layer MoS_2, respectively, and corresponding time-dependent plots have been provided in Ref. 44. Few-layer planar MoS_2 film has shown better stability

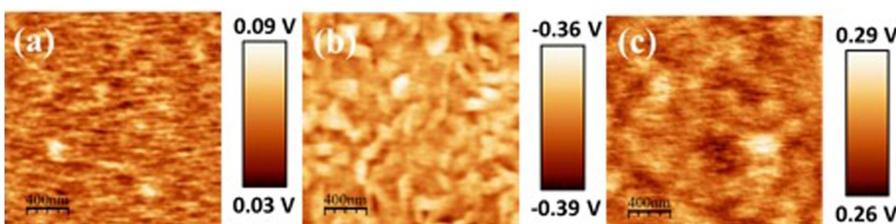

FIG. 6. Two-dimensional distributions of contact potential difference (V_{CPD}) between the tip and (a) few-layers, (b) 1L, and (c) EVTA MoS_2 thin films. In all the figures, the scale bar is 400 nm.

over ETVA MoS_2 film. The fluctuation in the ETVA emission current density might be due to the presence of different emission sites at exposed edges.

Ultra thin molybdenum films were sulfurized at two different reaction temperatures to yield few-layer and ETVA MoS_2 films, and single layer MoS_2 film was synthesized via the CVD method. The thickness of the few-layer film measured ~7–8 nm while presence of PL spectrum confirmed the monolayer deposition. A HRTEM image of ETVA MoS_2 revealed that the nanosize grains consisted of vertically aligned MoS_2 layers. A comparative study of cold cathode emission was performed on these few-layer and single layer MoS_2 films. The observed emission results affirmed that edge exposed MoS_2 exhibited $E_{to} \sim 4.5\,V/\mu m$ and emission current density $\sim 1\,m\text{-}amp/cm^2$ at $10\,V/\mu m$ and has good field emission stability that can be used in vacuum microelectronic applications. In comparison with other chemical synthesis methods reported so far to fabricate nanostructures of MoS_2, the sulfurization method is more efficient to modify surface topography, which in turn exhibits improved emission behavior.

A.P.S.G. and R.S.K. acknowledge the financial support from the DOE (Grant No. DEG02-ER46526). A.M.R. acknowledges the NSF (Grant No. 0841338). We also acknowledge the NSF for financial support (Cooperative Agreement No. EPS-01002410). We thank Mr. D. Barrionuevo for AFM measurements, and Dr. M. Ahmadi and Dr. M. Guinel for TEM work. We thank Dr. T. Som, Institute of Physics, Bhubaneswar, India, for extending his support to carry out the KPFM measurements.

[1]W. B. Choi, D. S. Chung, J. H. Kang, H. Y. Kim, Y. W. Jin, I. T. Han, Y. H. Lee, J. E. Jung, N. S. Lee, G. S. Park, and J. M. Kim, Appl. Phys. Lett. **75**(20), 3129 (1999).
[2]K. B. K. Teo, E. Minoux, L. Hudanski, F. Peauger, Jean-P. Schnell, L. Gangloff, P. Legagneux, D. Dieumegard, G. A. J. Amaratunga, and W. I. Milne, Nature **437**(7061), 968 (2005).
[3]H. Sugie, M. Tanemura, V. Filip, K. Iwata, K. Takahashi, and F. Okuyama, Appl. Phys. Lett. **78**(17), 2578 (2001).
[4]G. Z. Yue, Q. Qiu, B. Gao, Y. Cheng, J. Zhang, H. Shimoda, S. Chang, J. P. Lu, and O. Zhou, Appl. Phys. Lett. **81**(2), 355 (2002).
[5]W. A. de Heer, A. Châtelain, and D. Ugarte, Science **270**(5239), 1179 (1995).
[6]C. A. Spindt, C. E. Holland, A. Rosengreen, and I. Brodie, IEEE Trans. Electron Devices **38**(10), 2355 (1991).
[7]K. B. K. Teo, M. Chhowalla, G. A. J. Amaratunga, W. I. Milne, P. Legagneux, G. Pirio, L. Gangloff, D. Pribat, V. Semet, V. T. Binh, W. H. Bruenger, J. Eichholz, H. Hanssen, D. Friedrich, S. B. Lee, D. G. Hasko, and H. Ahmed, J. Vac. Sci. Technol., B **21**(2), 693 (2003).
[8]S. T. Purcell, P. Vincent, C. Journet, and V. T. Binh, Phys. Rev. Lett. **88**(10), 105502 (2002).
[9]X. Xu, C. Tang, H. Zeng, T. Zhai, S. Zhang, H. Zhao, Y. Bando, and D. Golberg, ACS Appl. Mater. Interfaces **3**(4), 1352 (2011).
[10]Cheng-K. Huang, Y. Ou, Y. Bie, Q. Zhao, and D. Yu, Appl. Phys. Lett. **98**(26), 263104 (2011).
[11]D. R. Shinde, P. G. Chavan, S. Sen, D. S. Joag, M. A. More, S. C. Gadkari, and S. K. Gupta, ACS Appl. Mater. Interfaces **3**(12), 4730 (2011).
[12]A. Datta, D. Mukherjee, M. Hordagoda, S. Witanachchi, P. Mukherjee, R. V. Kashid, M. A. More, D. S. Joag, and P. G. Chavan, ACS Appl. Mater. Interfaces **5**(13), 6261 (2013).
[13]L. Wang, C. Li, Y. Yang, S. Chen, F. Gao, G. Wei, and W. Yang, ACS Appl. Mater. Interfaces **7**(1), 526 (2015).
[14]A. K. Geim, Science **324**(5934), 1530 (2009).
[15]C. Lee, X. Wei, J. W. Kysar, and J. Hone, Science **321**(5887), 385 (2008).
[16]A. Malesevic, R. Kemps, A. Vanhulsel, M. P. Chowdhury, A. Volodin, and C. V. Haesendonck, J. Appl. Phys. **104**(8), 084301 (2008).
[17]S. Santandrea, F. Giubileo, V. Grossi, S. Santucci, M. Passacantando, T. Schroeder, G. Lupina, and A. D. Bartolomeo, Appl. Phys. Lett. **98**(16), 163109 (2011).
[18]U. A. Palnitkar, R. V. Kashid, M. A. More, D. S. Joag, L. S. Panchakarla, and C. N. R. Rao, Appl. Phys. Lett. **97**(6), 063102 (2010).
[19]B. Radisavljevic, A. Radenovic, J. Brivio, V. Giacometti, and A. Kis, Nat. Nanotechnol. **6**(3), 147 (2011).
[20]S. Das, Hong-Y. Chen, A. V. Penumatcha, and J. Appenzeller, Nano Lett. **13**(1), 100 (2013).
[21]M. Chhowalla and G. A. J. Amaratunga, Nature **407**(6801), 164 (2000).
[22]Y. Li, H. Wang, L. Xie, Y. Liang, G. Hong, and H. Dai, J. Am. Chem. Soc. **133**(19), 7296 (2011).
[23]D. Kong, H. Wang, J. J. Cha, M. Pasta, K. J. Koski, J. Yao, and Y. Cui, Nano Lett. **13**(3), 1341 (2013).
[24]A. P. S. Gaur, S. Sahoo, M. Ahmadi, M. J. F. Guinel, S. K. Gupta, R. Pandey, S. K. Dey, and R. S. Katiyar, J. Phys. Chem. C **117**(49), 26262 (2013).
[25]A. P. S. Gaur, S. Sahoo, M. Ahmadi, S. P. Dash, M. J. F. Guinel, and R. S. Katiyar, Nano Lett. **14**(8), 4314 (2014).
[26]Yi-H. Lee, L. Yu, H. Wang, W. Fang, X. Ling, Y. Shi, Cheng-T. Lin, Jing-K. Huang, Mu-T. Chang, Chia-S. Chang, M. Dresselhaus, T. Palacios, Lain-J. Li, and J. Kong, Nano Lett. **13**(4), 1852 (2013).
[27]G. Morell, A. González-Berríos, B. R. Weiner, and S. Gupta, J. Mater. Sci. - Mater. Electron. **17**(6), 443 (2006).
[28]R. V. Kashid, D. J. Late, S. S. Chou, Yi-K. Huang, M. De, D. S. Joag, M. A. More, and V. P. Dravid, Small **9**(16), 2730 (2013).
[29]Y. B. Li, Y. Bando, and D. Golberg, Appl. Phys. Lett. **82**(12), 1962 (2003).
[30]D. Varshney, A. V. Sumant, O. Resto, F. Mendoza, K. P. Quintero, M. Ahmadi, B. R. Weiner, and G. Morell, Carbon **63**, 253 (2013).
[31]C. Lee, H. Yan, L. E. Brus, T. F. Heinz, J. Hone, and S. Ryu, ACS Nano **4**(5), 2695 (2010).
[32]S. Sahoo, A. P. S. Gaur, M. Ahmadi, M. J. F. Guinel, and R. S. Katiyar, J. Phys. Chem. C **117**(17), 9042 (2013).
[33]B. Chakraborty, A. Bera, D. V. S. Muthu, S. Bhowmick, U. V. Waghmare, and A. K. Sood, Phys. Rev. B **85**(16), 161403 (2012).
[34]I. H. Campbell and P. M. Fauchet, Solid State Commun. **58**(10), 739 (1986).
[35]P. Parayanthal and F. H. Pollak, Phys. Rev. Lett. **52**(20), 1822 (1984).
[36]A. Splendiani, L. Sun, Y. Zhang, T. Li, J. Kim, Chi-Y. Chim, G. Galli, and F. Wang, Nano Lett. **10**(4), 1271 (2010).
[37]R. Stratton, Phys. Rev. **125**(1), 67 (1962).
[38]V. T. Binh and C. Adessi, Phys. Rev. Lett. **85**(4), 864 (2000).
[39]V. T. Binh, J. P. Dupin, P. Thevenard, S. T. Purcell, and V. Semet, J. Vac. Sci. Technol., B **18**(2), 956 (2000).
[40]M. W. Geis, N. N. Efremow, K. E. Krohn, J. C. Twichell, T. M. Lyszczarz, R. Kalish, J. A. Greer, and M. D. Tabat, Nature **393**(6684), 431 (1998).
[41]A. González-Berríos, F. Piazza, and G. Morell, J. Vac. Sci. Technol., B **23**(2), 645 (2005).
[42]C. Maragliano, S. Lilliu, M. S. Dahlem, M. Chiesa, T. Souier, and M. Stefancich, Sci. Rep. **4**, 4203 (2014).
[43]M. Kumar, T. Basu, and T. Som, J. Appl. Phys. **118**, 055102 (2015).
[44]See supplementary material at http://dx.doi.org/10.1063/1.4940306 for AFM, TEM, field effect transistor (FET) characteristics, and field emission stability results.